NPL Report MATC(A)51

Creep Properties of SnAgCu Solder in Surface Mount Assemblies

Jaspal Nottay, Milos Dusek,
Christopher Hunt,
Christopher Bailey and Hua Lu

August 2001

August 2001

Creep Properties of SnAgCu Solder in Surface Mount Assemblies

Jaspal Nottay, Milos Dusek and Christopher Hunt
Materials Centre
National Physical Laboratory
Teddington, Middlesex, UK, TW11 0LW

&

Christopher Bailey and Hua Lu
Centre for Numerical Modelling and Process Analysis
University of Greenwich
London, UK, SE10 9LS

ABSTRACT:

The move to lead-free solders has highlighted the need for materials property data relating to these new solders. Such data are required to model joint performance and to predict service life under long-term thermo-mechanical fatigue. In consequence, some creep property data of arguably the most attractive lead-free solder, SnAgCu, have been determined in this work using samples and solder joints whose geometries and sizes were representative of today's surface mount technology. These data were compared to those from the literature on bulk specimens (specifically for SnPb and SnAg solders) using a constitutive model developed by Darveaux. The comparison not only suggested there might be significant differences between the creep properties of the alloys, but also highlighted the importance of joint area and geometry in the determination of the creep behaviour of the solders.

ISSN 1473-2734

National Physical Laboratory
Queens Road, Teddington, Middlesex, TW11 0LW

Approved on behalf of the Managing Director, NPL
by Dr C Lea, Head, Materials Centre

CONTENTS

1 INTRODUCTION

There is general agreement now that whatever the drivers, be they legislative, technological or commercial, lead-free soldering will become the industrial norm in the next few years. However, one of the key concerns in embracing lead-free soldering technologies is the lack of reliability data relating to the solder joints under the various service conditions existing in a range of industrial applications. Hence an increased emphasis is being placed on the use of modelling to predict service performance and life. Such a move towards a greater use of modelling is also being spurred by the increasing cost of practical experiments, the wide choice of lead-free solders, the variability of joint geometries, and the increased capability of modelling and the reduced cost of computing time.

In order to make effective use of modelling it is essential to have a good understanding of the thermo-mechanical behaviour of the new lead-free solder alloys, the availability of appropriate mathematical descriptions, and reliable materials property data. But such data are sparse, even for the most attractive of the lead-free solders, SnAgCu. In order to predict the lifetime of solder joints a number of factors need to be understood, including

- solder joint three dimensional profile
- heating or soldering regimes and the resultant microstructure
- temperature and loading regimes during thermal cycling

In the case of the new families of lead-free solders few data on the creep properties are known, and studies are urgently required to ascertain these data at various strain rates and temperatures. Such thermo-mechanical properties can be generated using appropriate mathematical descriptions and accurate experimental data. In the simplest form this can be achieved using a typical creep bulk solder specimen and a constant strain rate, and measuring the extension of the specimen with time. Indeed, previous work reported in the literature (3) has involved such bulk solder specimens, since they do have the expedient advantage that the test methods are readily available.

For modelling joints typical of surface mount (SM) product, however, this approach is flawed, and any data will have little correlation with the performance of the solder in these very small joints. Therefore a different approach is required that provides data from joint geometries mimicking today's SM technology that will have a high degree of industrial relevance. Such an approach has been used in this work in which the testing system, comprising a double lap joint arrangement, provided deformation of the solder which followed relative in-plane displacement of the bonded strip comparable to that experienced by real SM solder joints.

2 EXPERIMENTAL

When modelling thermo-mechanical fatigue in electronics assemblies it is the mismatch of thermal expansion (CTE) within a typical assembly that is of major concern. Under

thermal cycling these differences produce substantial cyclic strains within the solder leading to fatigue by a process of crack initiation and propagation (1). The creep behaviour of soft solders can result in excessive deformation with thermal cycling under strain-controlled conditions, producing crack initiation and propagation in the solder. The microstructural characteristics of lead-free alloys suggest that there is a coarsening effect of the grains when they are subjected to thermal cycling (2), which can also result in crack formation.

In modelling the behaviour of solder joints three important factors need to be considered, viz: the joint filet size and shape, the component stand-off height, and the materials properties of the solder (i.e. Young's modulus and Poisson's ratio).

In terms of the first two factors, different component types produce solder joints with various, complex, joint profiles that often contain curvatures on all sides. Such profiles are sensitive to a number of process variables, and this variability can make reliability prediction difficult. As mentioned above, computer modelling can aid in obtaining a fuller understanding of reliability issues as functions of these many variables.

When the dimensions of the sample approach that of the grain size, a situation that exists in many solder joints in today's electronics assemblies, it is to be expected that the behaviour of the solder will markedly change. Therefore, test samples that mimic real SM product are essential. A convenient method of achieving this is to use a lap joint arrangement, and this has been used in the present work. The stresses associated with a single lap shear solder joint are similar to those that occur in a typical SM solder joint. The component is represented by one part of the lap, the solder is represented by the intermediary part, and the pad/board the third part – see Figure 1 for a schematic of a typical sample. A symmetrical build-up of four joints helps to provide essentially shear forces.

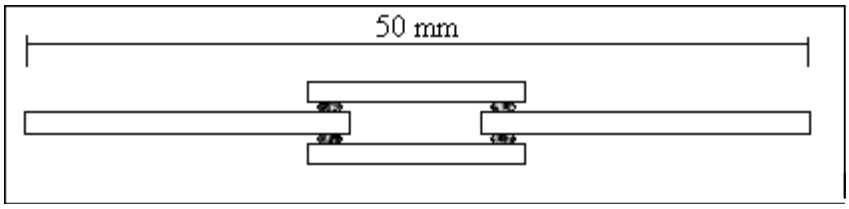

Figure 1. Schematic of a typical joint.

2.1 Assembly and Materials

The solder used in this experiment was SnAgCu in paste form, with a nominal composition of Sn (95.8%), Ag (3.5%) and Cu (0.7%). This solder is attracting considerable attention as a Pb-free replacement for the conventional SnPb solder. The substrate material was FR4 epoxy laminate with a bare copper finish.

To manufacture the joints, paste was printed on to the FR4 laminate and then soldered using a conventional reflow oven. The dimensions of the specimen produced when

manufactured was 50 x 3 x 2 mm. Figure 2 shows a manufactured test specimen in plan view, and Figure 3 shows a sample mounted in the test machine.

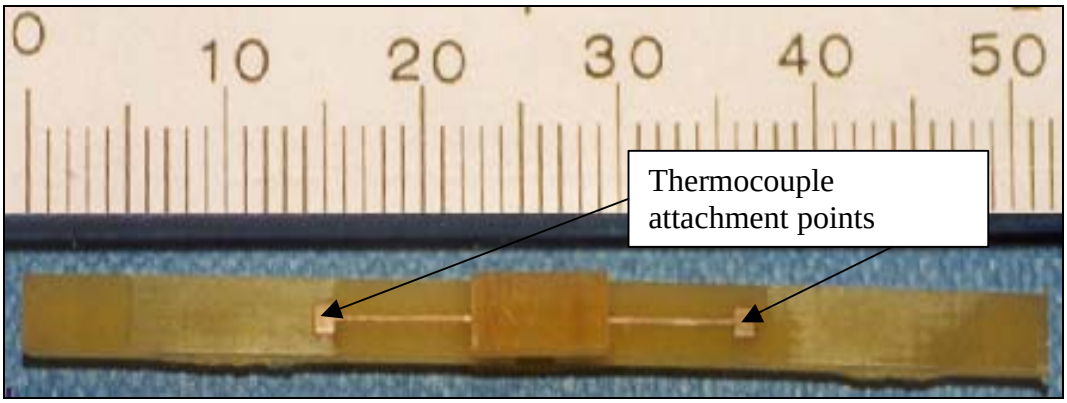

Figure 2. Manufactured test specimen displaying the double-lap joint in the centre region.

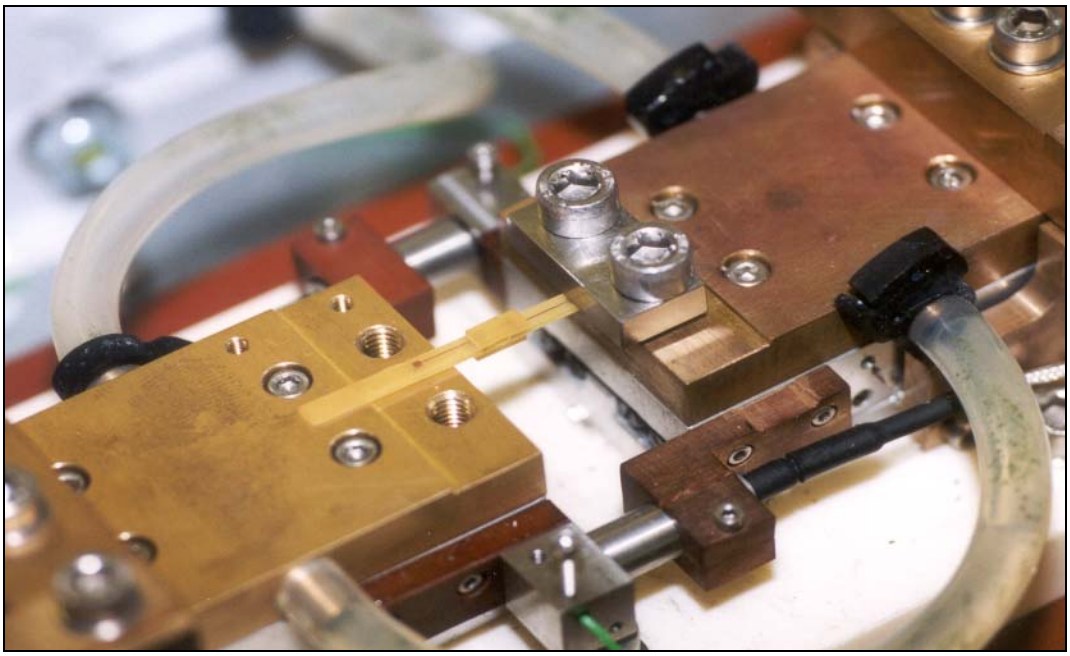

Figure 3. Specimen loaded within the ETMT machine.

2.2 Testing

The samples were tested in a small instrument, the Electro-Thermal Mechanical Test system (ETMT), which has been developed at NPL(4). The ETMT machine comprises a mechanical loading assembly that includes a grip system suitable for small-scale samples, and includes a load cell and linear displacement transducers (located on either side of the sample). A computer controlled motor system is used for load application in

the horizontal plane. Various types of tests can be conducted including strength tests, creep tests and thermo-mechanical fatigue (TMF) tests.

Constant load creep tests were conducted at various applied loads at 22, 75 and 125°C. The loads selected were in the range 10-30 Newtons. Table 1 gives specific loads applied at the three temperatures.

Table 1. Temperature and Loads in Creep Tests

Test type	Temperature	Load (Newtons)
Constant load creep test	22°C	10, 20, 25, 30
	75°C	10, 20, 30
	125°C	10, 20, 30

For tests at higher temperatures and at 50 N, the joints failed immediately.

The method used to heat the specimen within the ETMT machine consisted of a stainless steel tubular furnace attached between the clamps with a computer controlled DC heating power supply (200 amps). Thermocouple wires were sited in the joint region (Figure 2), and were attached using high temperature solder along the exposed pads of the specimen shown in Figure 2. Once the temperature had stabilised the load was applied and the displacement (i.e. extension) recorded. The shear stress was calculated taking the load and the area of the four solder joints into account. The shear stress values are given in Table 2.

Table 2. Force and shear stress values.

Load (N)	Shear stress (MPa)
10	2.48
20	4.97
25	6.21
30	7.45

3 RESULTS

3.1 Extension and Time Plots.

The displacement-time curves are plotted in Figures 4 and 5 for tests carried out at 22 and 125°C. In Figure 5 the data are plotted on a logarithmic scale for clarity.

Referring to Figure 4, at the lower applied stresses (2.48, 4.97 MPa) the elongation increased gradually with time. The amount of displacement occurring was in the region of 0-10 micrometers. However, as the stress was increased to 6.21 MPA a transition occurred, in which initially the sample extended by about 30 micrometers and continued at a high rate of extension over time. Whilst the initial extension is

commonly called “primary” creep. The next characteristic part of the curve, seen initially as a decrease in the creep rate and then a constant value, is known as “secondary” creep or steady state creep. The last part of the curve is known as the “tertiary” creep. In this latter area there is a rapid increase in extension as sample failure occurs. Secondary creep is representative of the creep properties of solder under thermal cycling conditions once initial strain hardening has occurred (at the primary creep area) [5]. This behaviour has been seen in previous creep tests conducted at NPL and elsewhere on solders [1,3,4].

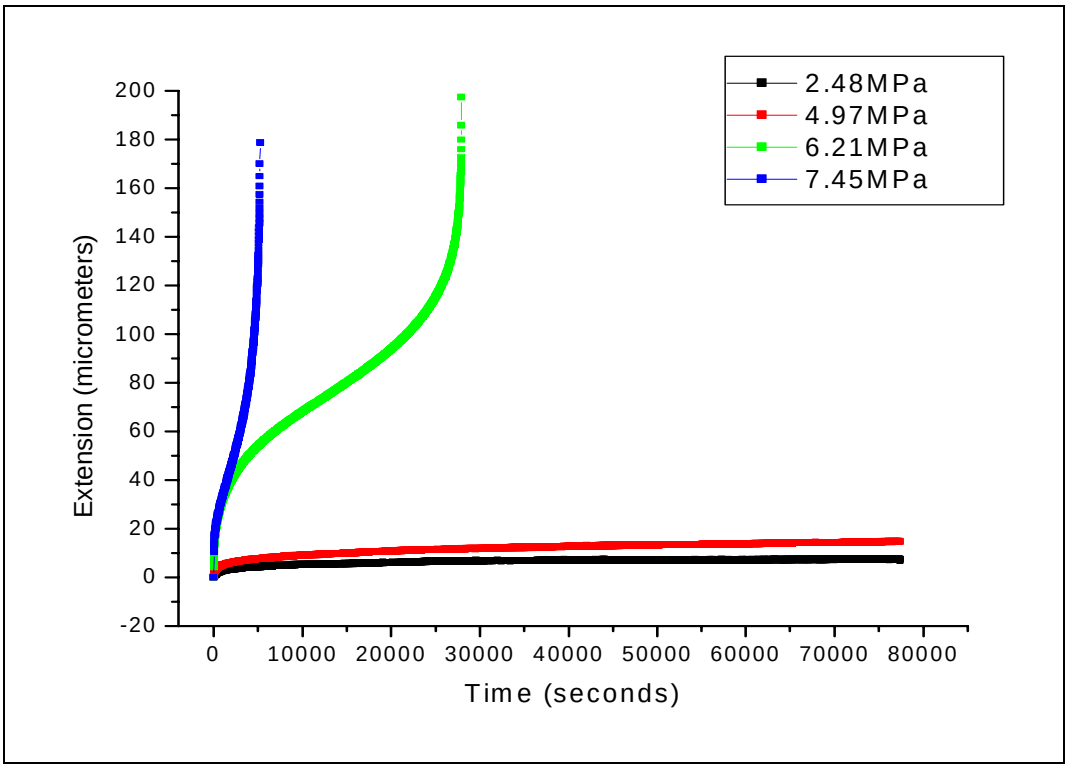

Figure 4: Extension-time plots for SnAgCu solder joints in shear at 22^0C

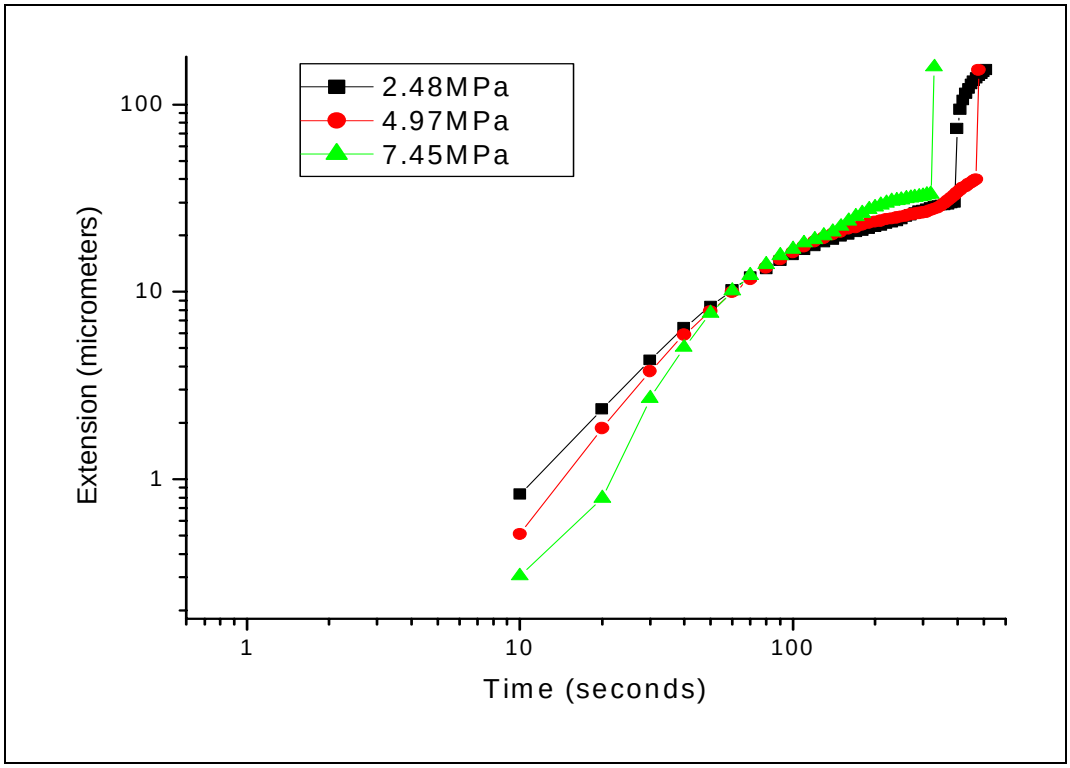

Figure 5: Displacement-time plots for SnAgCu solder joints in shear at 125°C.

At 125°C, the results show rapid displacement with time at all three stress levels used, compared to the results obtained at 22°C for the same applied stress levels. The sample arrangement used here results in predominantly pure shear stress and strain For modelling purposes the stress-strain behaviour must be known individually in each axis.. To achieve this, the experimental results are converted to effective stress and strain and these are then used to formulate the appropriate constitutive law used in the modelling analysis. From the extension-time plots the effective stress and strain were calculated in the steady-state creep regime. The Von Mises equation (eqn 1) is a definition of the effective stress. It simply states that in a general stress state, the effective stress can be calculated from the 6 stress components. Tensile or pure shear tests are two special cases when there is only one stress component, but the effective stress can be calculated in the same way. The conversion of tensile or pure shear stress into effective stress is needed in the creep constitutive law (discussed later, and given in equation 7).

To calculate the effective stress within the joint this value must be converted into a tensor by using the Von Mises' equation shown below.

$$\sigma_e = \frac{1}{\sqrt{2}}\sqrt{(\sigma_x-\sigma_y)^2+(\sigma_y-\sigma_z)^2+(\sigma_z-\sigma_x)^2+6(\tau_{xy}{}^2+\tau_{yz}{}^2+\tau_{zx}{}^2)} \quad (1).$$

In calculating the stress, since pure shear stress τ_{xy} is non-zero, the effective stress is the shear stress x square root of 3. The reason we have to convert the tensile or pure shear stress into effective stress is that it is needed in the creep constitutive law.

The effective strain and effective stress can then be plotted for each experiment at various stresses and different temperature regimes used. Figures 6, 7 and 8 correspond to the tested temperatures [6].

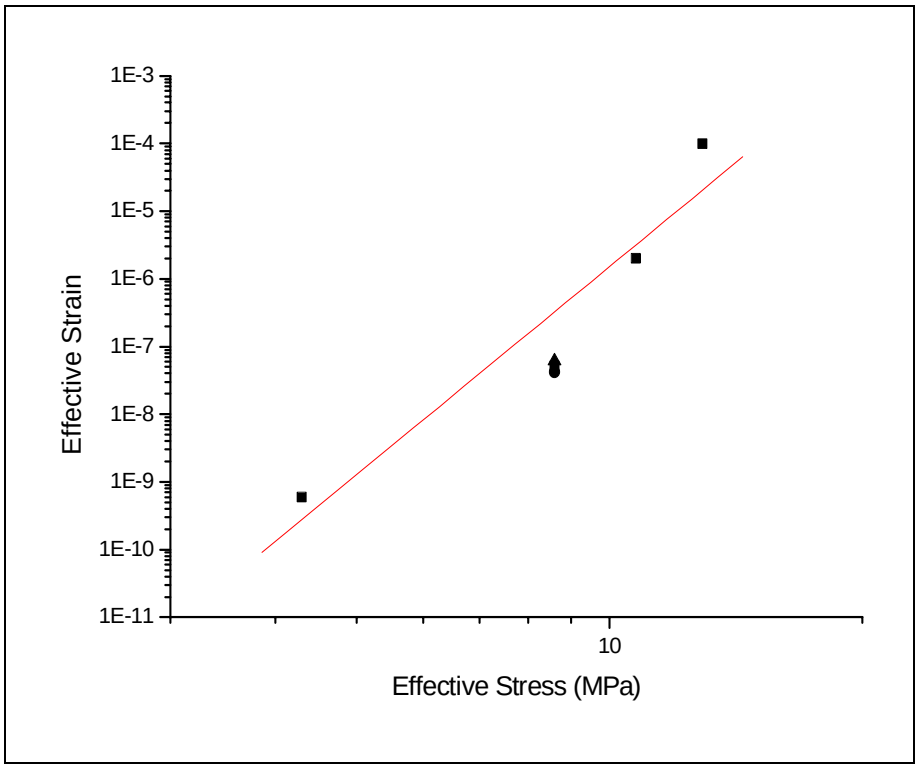

Figure 6: Steady state creep plot at 22°C for SnAgCu

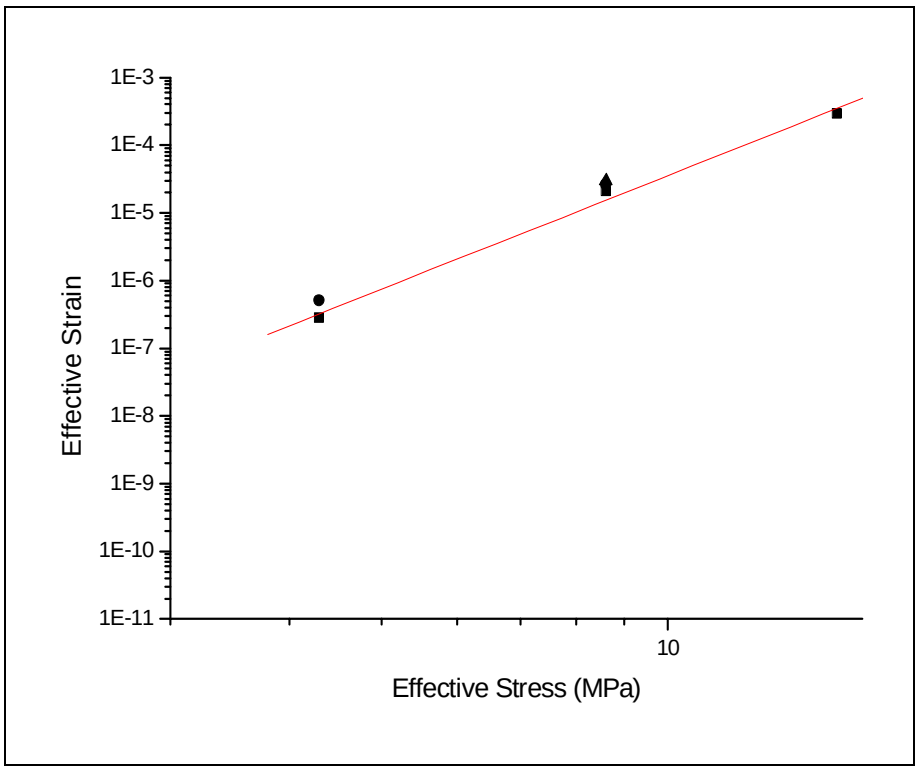

Figure 7. Steady state creep plot at 75°C for SnAgCu

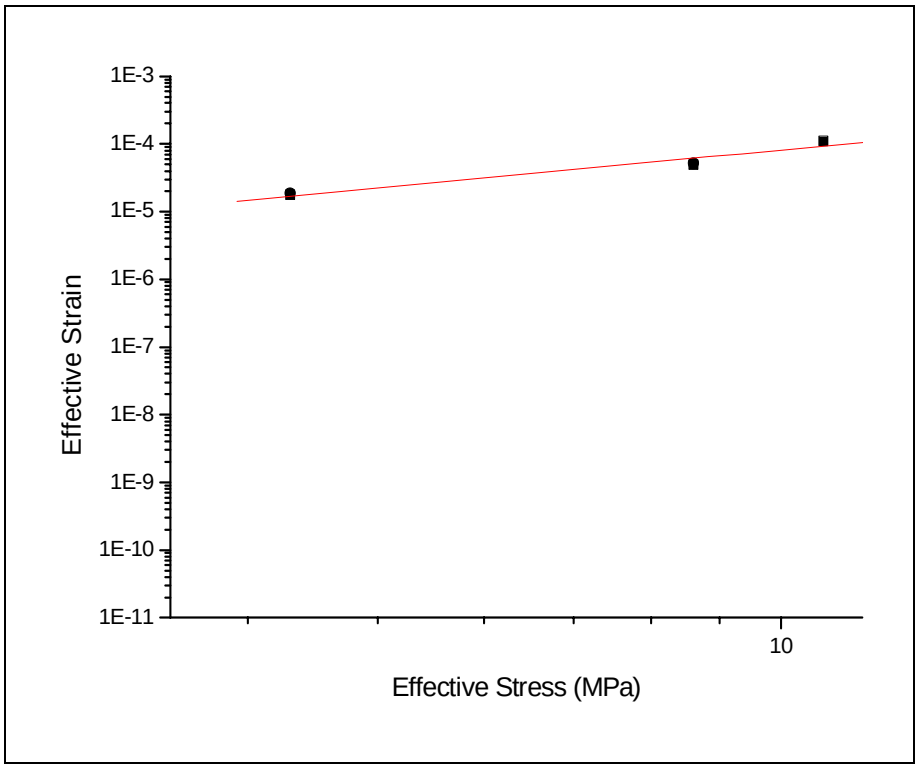

Figure 8. Steady state creep plot at 125°C for SnAgCu

After averaging for each experimental condition, all the data are replotted in Figure 9.

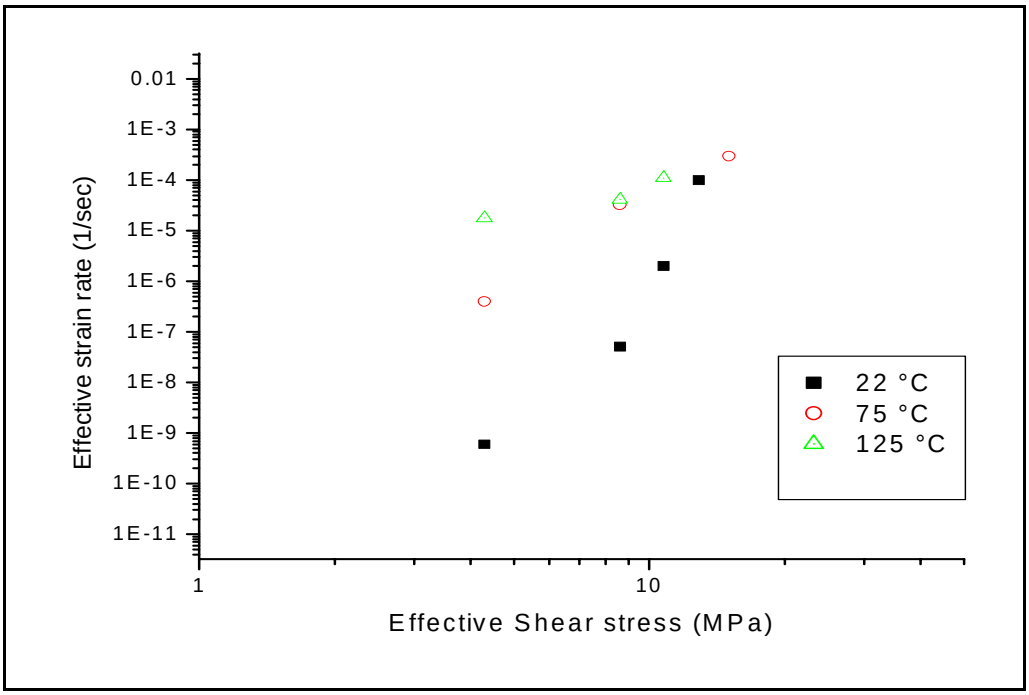

Figure 9. Steady state creep plot at all temperatures.

4 DISCUSSION

4.1 Constant Stress Creep Tests.

Figures 6, 7 and 8 represent the results from the creep tests that were conducted. A rise in temperature mainly affects the creep strain at lower stresses producing higher strain values for a given stress. At these stress levels the solder is vulnerable to increased levels of creep with changes in temperature, producing strains two orders of magnitude higher for every increase of 50°C. At high temperatures the samples failed rapidly when compared with lower temperatures due to this large change in the creep properties in the solder. This behaviour can be seen to occur in the extension-time plots shown in Figures 4 and 5. Figure 9 demonstrates that the solder alloy suffers a large amount of creep at high temperatures and high shear stress. However, at this high shear stress the strain is less dependent on temperature.

4.2 FR4 Creep Tests

When considering the validity of the experiments the material properties of the substrate, in this case FR4, are very important. An experiment was conducted to ascertain the behaviour of FR4 samples in creep testing. This was achieved by testing the FR4 material and calculating the extension that would occur, and comparing it to the extensions observed during the actual creep tests using solder. The results of this test are presented in Figure 10.

The data show the extension-time plots for the earlier SnAgCu solder at 2.48 MPa and that of the FR4 material at a stress of 14.8 MPa, at the same temperature (25°C). The stress of 14.8 MPa was significantly higher than the stress applied to the solder. Hence, the assumption that the deformation is in the solder is substantiated, and any effect due to the substrate can be discounted.

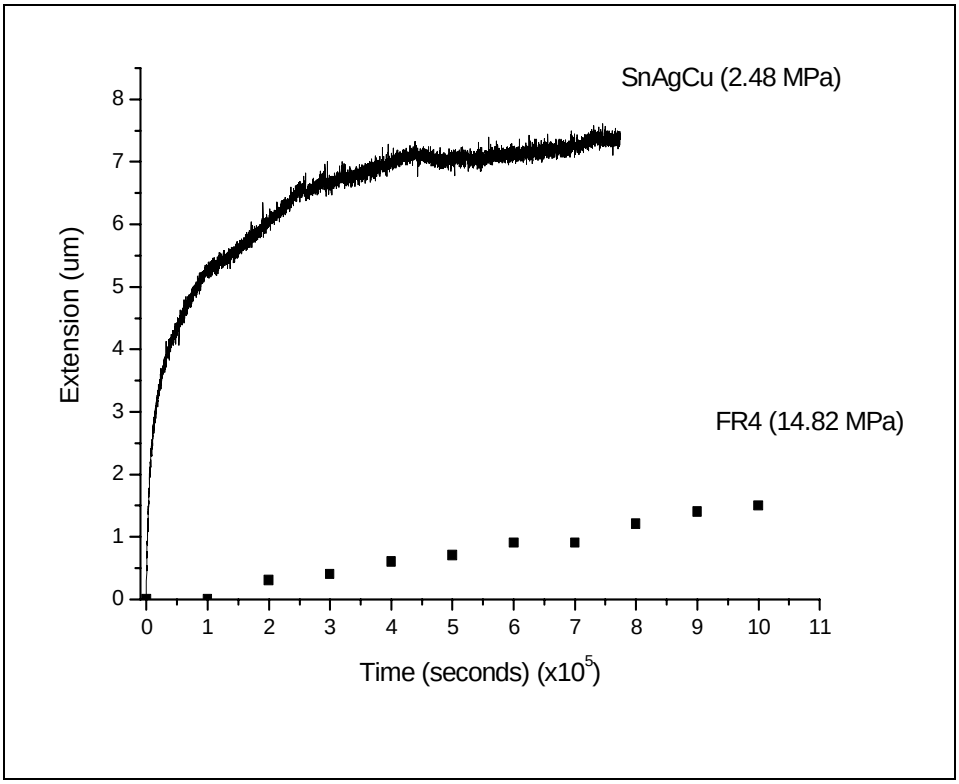

Figure 10. A comparison of extension of SnAgCu solder and FR4 substrate material.

4.3 Discussion of Experimental Creep Data

This preliminary study has shown that there are a number of issues with measurements of creep on realistic sized solder joints. Steady state creep rate has a maximum value of around 10^{-4}. The study has shown that the selection of applied stress was not ideal and that more work is required at lower stresses. Nonetheless some clear conclusions can be drawn regarding the creep behaviour of this SAC alloy. The data at 22°C and shear stresses less than 10 MPa are similar to those in the literature, but at the higher temperatures the creep rate is significantly higher. More data are required at intermediate temperatures to establish the trend in creep rate with temperature.

4.4 Comparison of Creep Models

One of the main reasons for generating creep data is to facilitate meaningful modelling the behaviour of solders. The models must of necessity make assumptions about the material properties if any useful solutions and conclusions are to be drawn. Three models that are generally applicable to solders have been considered here.

4.4.1 Darveaux Model

Within solder, the steady state creep equation [7] is not generally achieved when a stress is applied to a solder joint. A certain amount of transient creep will occur. As the stress is applied transient creep normally occurs before attaining a steady state. According to *Darveaux et al* the transient creep at constant stress and temperature can be described as:

$$\varepsilon_c = \frac{d\varepsilon_s}{dt} t + \varepsilon T (1 - \exp(-B \frac{d\varepsilon_s}{dt} t)) \quad (2).$$

Where ε_c is the creep strain, $d\varepsilon_s / dt$ is the steady state creep rate, εT is the transient creep strain, and B is the transient creep coefficient. Taking the time derivative leads to:

$$\frac{d\varepsilon_c}{dt} = \frac{d\varepsilon_s}{dt} (1 + \varepsilon TB \exp(-B \frac{d\varepsilon_s}{dt} t)) \quad (3).$$

Where $d\varepsilon_c / dt$ is the instantaneous creep rate and $d\varepsilon_s / dt$ is the steady state creep, rate. This relation shows that when t=0 the instantaneous creep rate will equate to $(1+\varepsilon TB)$ times greater than at steady state.

Darveaux et al have principally used the equations above to calculate successfully the creep behaviour of SnPbAg and other solder alloy combinations. This series of equations is commonly known as the *Darveaux model*. As mentioned before, there are other models, which can also be used. In the next Section these will be examined in order to assess which best applies.

4.4.2 Qian and Liu Model

The Qian and Liu model is a new unified visco-plastic model that has been used recently (1997) to predict the viscoplastic and creep behaviour of eutectic solders. [8]. It has been found by Qian and Liu to have a good correlation to experimental data obtained by them. This has been attributed due to the principle of rate-temperature-dependant properties when creep testing solders. The main difference in this model when compared to others is that it takes into account the creep damage evolution in the tertiary stage of creep testing for calculating the life prediction of a solder joint. This model takes into account of back stresses and kinematic hardening during cycle loading, and is equipment specific, using a purpose built six-axis tester. Due to the complexity of specimen geometry required and the many different operating variables this specific model cannot be used by NPL.

4.4.3 Kariya and Otsuka modified Coffin-Manson Model

Recent work concerning Sn-3.5Ag-X solders alloys by Kariya and Otsuka [1], concentrates on a modified version of the Coffin-Manson equation to predict the

fatigue and creep properties of these alloy types. Previous work conducted on an Sn-3.5Ag-Bi alloy by Kariya and Otsuka found that the fatigue life was dominated by the fracture ductility of the alloy and obeyed the tailored version. This version is represented in the equation below:

$$(\frac{\Delta\varepsilon_p}{2D}).N_f^{\alpha} = C \qquad (4)$$

where $\Delta\varepsilon_p$ is the plastic strain range, N_f is the fatigue life, D = ln {100/100-RA}, where RA is the percentage reduction in area and α, C are non-dimensional constants. This modified form of the equation can apparently be applied to ternary Sn-Ag-X alloys including SnAgCu. It was found that the fatigue life of these alloys were dominated by the ductility of each alloy and not by the amount of the third element present within an alloy type. This equation can be compared to the original Coffin-Manson law:

$$N_f.\Delta\varepsilon_{pl}^{n} = const. \qquad (5)$$

where N_f is the number of cycles to failure, Δ_{pl} is the plastic strain induced during each cycle and n is the damage exponent.

Extensive work conducted by Kariya and Otsuka concluded that the fatigue life of Sn-Ag-X solders including SnAgCu ternary alloy was found to be dominated by their individual fracture ductility irrespective of the kind of alloy. The ductility of these alloys was found using a static tensile test and from the information gathered through experimentation. The Coffin–Manson equation was furthermore modified to the following form:

$$(\frac{\Delta\varepsilon_p}{2D}).N_f^{0.51} = 0.42 \qquad (6)$$

with this relation once the values for $\Delta\varepsilon_p$ and D are known the fatigue life could be predicted for Sn-Ag-X systems. The work conducted Kariya and Otsuka is directly related to what the current work is trying to achieve in calculating the creep properties of SnAgCu alloy. Plotting the plastic strain range against the fatigue life, Nf, normally represents Coffin-Manson plot [1], and these are used to indicate the fatigue/ creep properties of solder alloys. However, the main drawback with this model would be in the calculation of the reduction in area for the test vehicle used here, which is in essence a 4-joint double lap. The presence of 4 individual joints of a relatively small cross-section confers considerable complexity on the determination of the reduction in area.

4.4.4 Model Conclusions

Examining all the models for suitability has resulted in the selection of the Darveaux model. Since this model is directly applicable to our current experimental set-up we can readily calculate the values required for the constitutive equation. This model has

also been applied to ternary systems, similar to the SnAgCu solder used. The Qian and Liu model is currently restricted by the fact that it requires geometry specific samples. It also takes account of specific material constants that can only be calculated using time consuming computation. As mentioned above the modified Coffin-Manson equation as used by *Kariya et al* relies on geometry changes, which would be impossible to measure without changing the samples used in this work.

4.5 Comparison of Data with Darveaux Model

The vast majority of experimental data on solder joints is based on bulk samples. The experimental data obtained in this analysis are compared with previous work conducted by R. Darveaux *et al* [7] on BGA type solder specimens. The data from Darveaux, as typical from the literature, and is for scalar stresses, that is specimen geometry effects are normalised. To convert what is actually a tensor stress to a scalar stress, the method employed by Darveaux was used [6]. This actually takes the form of a constitutive *equation 7*, which was fitted by Darveaux to his SnPb data, and here to the experimental SnAgCu data.

$$\frac{d\varepsilon_{cr}}{dt} = A \times \sinh^{n}(\alpha\sigma_{e}) \exp(\frac{-Q}{RT}) \qquad (7)$$

Where: $d\varepsilon_{cr}/dt$ is the scalar creep strain rate,
A is the pre-exponential factor,
T is absolute temperature,
R is the gas constant,
σ_e is the Von Mises effective stress,
Q is the activation energy and
α and n are material dependent constants.

The fitted coefficients for equation 7 for the three alloys, which are given in Table 3, can be used to calculate the stress-strain behaviour over the stress range of 4 to 58 MPa. The calculated results are and given in Table 4 and plotted in Figure 11.

Table 3. Fitted coefficient values for equation 7.

SnAg	SnAgCu	SnPb
A=9E+05	A=9.62E+04	A=9.62E+04
α=0.06527 MPa^{-1}	α=0.092538 MPa^{-1}	α=0.087 MPa^{-1}
$_n$ =5.5	$_n$ =15.631	$_n$ =3.3
Q=8690.37R	Q=8060.166R	Q=8058.37R

Table 4. Stress and strain behaviour for SnAg, SnAgCu and SnPb

Solder	**SnAg**	**SnAgCu**	**SnPb**
Stress (MPa)	Strain rate	Strain rate	Strain rate
4	9.07E-12	1.03E-10	5.77E-09
10	1.93E-09	2.97E-07	1.66E-07
16	4.58E-08	2.60E-05	1.43E-06
22	5.93E-07	8.02E-04	9.19E-06
28	6.1E-06	1.59E-02	5.39E-05
34	5.69E-05	2.54E-01	0.00030
40	0.000508	3.64	0.0017
46	0.004448	4.91E+01	0.0097
52	0.03861	6.44E+02	0.054
58	0.333	8.30E+03	0.304

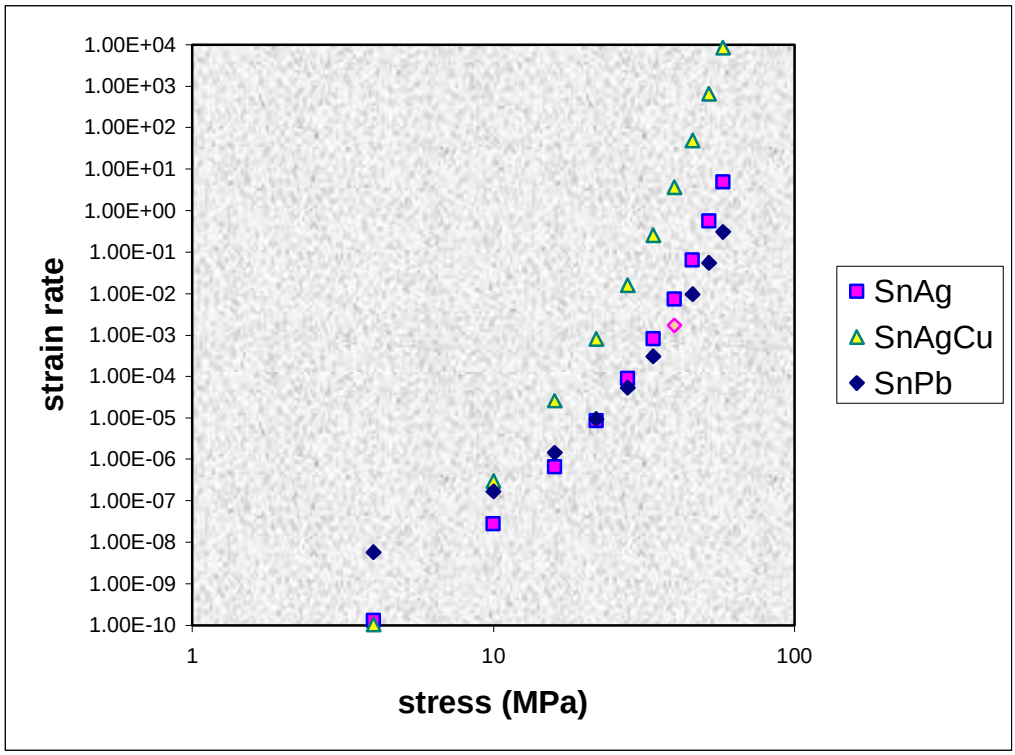

Figure 11. Creep properties of 3 different solder systems.

The stress-strain data for SnAgCu, SnPb and SnAg solder at 25°Care presented in Figure 11. The plotted data for SnPb and SnAg were obtained from the previous work by R. Darveaux [7], and the SnAgCu data were derived from the present work. The values for SnAgCu are markedly different to those of the other two materials. At low stresses the alloy has a strain rate comparable to SnAg, however at high stresses the strain rate of the SnAgCu alloy is very much higher than the strain rate of either SnAg or SnPb. The cause of this difference could be geometry related. The specimens used in the present work were modelled on actual component size and pad geometries, whereas the data from other alloys relate to BGA size solder joints. This difference

would suggest that the joint area, geometry and test are crucial in the determination of the creep behaviour in solder alloys.

5 CONCLUSIONS

This study has investigated the creep properties of the ternary solder alloy SnAgCu joint properties using geometry-specific samples that are representative of surface mount solder joints. The results have been compared with the creep properties of bulk solder specimens of SnPb and SnAg using similar constitutive laws. This investigation has shown that there is a significant difference between the SAC results and those of SnPb and SnAg. This difference is attributed largely to sample geometry differences. A clear recommendation is to compare data from samples of the same geometry using the different solder alloys. Any modelling using these SAC data, and comparing then it with SnPb data will therefore have to take sample geometry into account. Furthermore, it is recommended that the effect of solder fillet size be assessed.

6 ACKNOWLEDGEMENTS

This work was carried out as part of a project in the Measurements for the Processability of Materials (MPM7.3) Programme of the UK Department of Trade and Industry. The authors are also grateful to Martin Wickham and Bryan Roebuck for the useful discussions and information on solder alloy behaviour through out the work.

7 REFERENCES

[1] Kariya, Y. Otsuka, M. Mechanical fatigue characteristics of Sn-3.5Ag-X (X=Bi, Cu, Zn and In) Solder Alloys, Journal of Electronic Materials, Vol. 27, No. 11, 1998. pp 1229-1235.

[2] Dusek, M. Nottay, J. Hunt, C. The use of Shear testing and Thermal Cycling for Assessment of Solder Joint Reliability. NPL Report CMMT (A) 268, June 2000, Teddington.

[3] Kuo, C.G. Sastry, S.M.L. Jerina, K.L. Tensile and creep properties of in-situ composite solders. Microstructures and Mechanical Properties of Aging Materials, The Minerals, Metals and Materials Society, 1993. pp 409-412.

[4] Mummery, P. Foroodian, M. Roebuck, B. Thermomechanical Fatigue of Solders. NPL Report CMMT (D) 202, March 1999, Teddington.

[5] Rensselear Polytechnic Institute (RPI), Creep Information Datasheets 22-27. 110 8th St., Troy, NY 12180 (518) Reference: 276-6000

[6] Darveaux, R. Banerji, K. Constitutive relations for Tin-based Solder Joints. I.E.E.E. Transactions on components hybrids and manufacturing technology. Volume CHMT-15, 1992, pp 1013-1024.

[7] Darveaux, R. Solder Joint Fatigue Life Model, Design and Reliability of Solders and Solder Interconnections. The Minerals, Metals and Materials Society, 1997, pp 213-218.

[8] Ren W., Qian Z.and Liu S. Thermo-mechanical Creep of Two Solder Alloys: Electronic Components and Technology Conference, 1998, pp 1431-1437.